frontiers | Frontiers in Earth Science

TYPE Original Research
PUBLISHED 04 January 2023
DOI 10.3389/feart.2022.1062580



OPEN ACCESS

EDITED BY
Yu Song,
China University of Mining and Technology, China

REVIEWED BY
Bo Zhao,
Taiyuan University of Technology, China
Liu Xueying,
Huaqiao University, China
Xin-Bo Zhao,
Qingdao University of Technology, China

*CORRESPONDENCE
Di Wu,
wudi202@126.com

SPECIALTY SECTION
This article was submitted to Economic Geology, a section of the journal Frontiers in Earth Science

RECEIVED 06 October 2022
ACCEPTED 01 December 2022
PUBLISHED 04 January 2023

CITATION
Yu Y, Liu J, Yang Y, Wu D, Zhai W and Miao F (2023), Experimental study on coal seam permeability enhancement and $CO_2$ permeability caused by supercritical $CO_2$.
*Front. Earth Sci.* 10:1062580.
doi: 10.3389/feart.2022.1062580



# Experimental study on coal seam permeability enhancement and $CO_2$ permeability caused by supercritical $CO_2$

Yongjiang Yu[1], Jingjing Liu[1], Yuntao Yang[1], Di Wu[2]*, Wenbo Zhai[2] and Feng Miao[2]

[1]School of Mining, Liaoning Technical University, Fuxin, China, [2]School of Mechanics and Engineering, Liaoning Technical University, Fuxin, China

Permeability is one of the most important parameters for characterizing fluid flow and production from reservoirs. In this paper, experimental studies on the percolation, permeability, and adsorption of supercritical $CO_2$ in coal seams were carried out, taking into account the effects of injection pressure and temperature, comparing the changes in longitudinal wave velocity of specimens before and after the tests, and analyzing the permeability effect of supercritical $CO_2$ on raw coal specimens. The test results showed that when the volume stress was 36 MPa, the permeability of supercritical $CO_2$ in coal increased by 93%, on average, compared with that of $CO_2$. The modified D-R model was used to fit the adsorption data, and it was found that the excess adsorption capacity of supercritical $CO_2$ by coal decreased with increased pressure, with a maximum value of approximately 8 MPa. When the temperature increased by 10°C, the adsorption capacity decreased by 8.3%, on average. In the subcritical $CO_2$ state, the trend of excess $CO_2$ adsorption in coal was consistent with that of absolute adsorption, which was 16% higher than that of excess adsorption, on average. After the action of supercritical $CO_2$, the propagation velocity of the longitudinal wave in the sample decreased significantly, indicating that supercritical $CO_2$ can effectively promote the development of pores and fractures in the coal sample, with an obvious anti-reflection effect on the coal seam and the best permeability enhancement effect at 35°C.

KEYWORDS

**supercritical $CO_2$, permeability, adsorption capacity, longitudinal wave velocity, permeability enhancement**

## Introduction

As coal resources continue to decrease, efficient mining of coal-bed methane becomes important (Jia et al., 2012). China's coal-bed methane resources are mainly located 1,500-3,000 m underground, and existing coal-bed methane mining technology is limited by factors such as high temperature and high ground stress in deep coal seams, although these characteristics

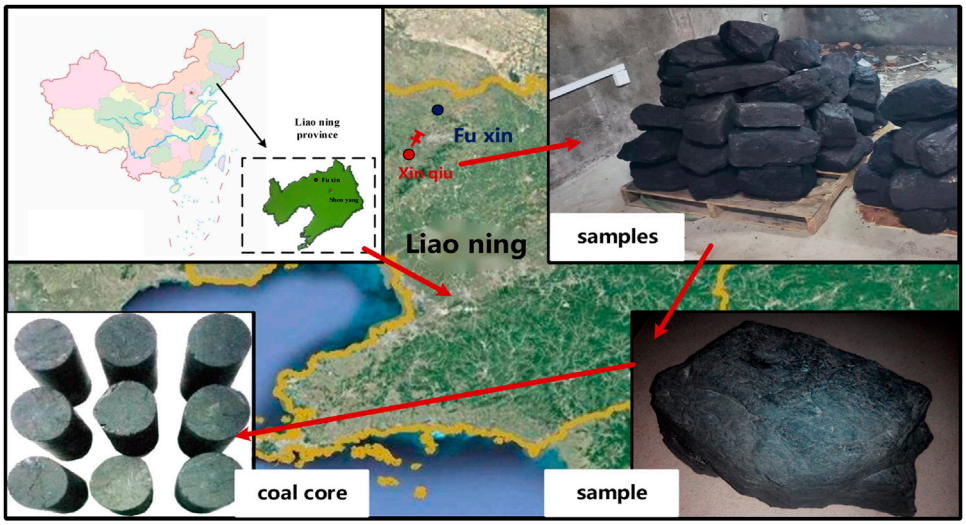


FIGURE 1
Coal samples.

are not universal (Feng, 2008). In recent years, methods for the recovery of enhanced stored coal-bed methane using $CO_2$ ($CO_2$ - ECBM) have received increasing attention (Reucroft and Patel, 1986; Reucroft and Sethuraman, 1987; Qin, 2005; Wu and Zhao, 2005). This method is based on good fluidity and zero surface tension of supercritical $CO_2$, which can not only significantly improve the recovery of coal-bed methane but also store $CO_2$ in coal seams to reduce the greenhouse effect.

In recent years, many scholars have studied the seepage and adsorption properties of coal on $CO_2$. (Xu et al., 2017) explored the sensitivity of the response of coal rock permeability to changes in stress by testing $CO_2$ in the coal seam and found that the greater the stress, the less sensitive the corresponding force of coal sample permeability. Through the $CO_2$ isothermal adsorption test, it has been found that the $CO_2$ isothermal adsorption curve reaches a maximum value near the critical pressure (7.38 MPa) and then gradually decreases with increased adsorption pressure (Wu et al., 2019; Wu et al., 2021; Miao et al., 2022). Ma et al. (2015) studied the adsorption capacity of coal for different gases and found that the capacity for adsorption of $CO_2$, $CH_4$, and $N_2$ decreased sequentially. Tang et al. (2004) confirmed the superiority of $CO_2$ in competitive adsorption with $CH_4$ through the experimental study of adsorption isotherms of $CO_2$–$CH_4$ binary gas. He et al. (2018) studied the expansion deformation of $CO_2$ adsorption of coal bodies of different coal grades and concluded that expansion deformation decreased with increased coal grades under the same amount of $CO_2$ adsorption. By comparing multiple adsorption models, it was found that the modified D-R model could better describe the trend of supercritical $CO_2$ adsorption in coal (Sakurovs et al., 2007; Richard et al., 2008; Wu et al., 2018a). Sun et al. (2013) studied the seepage law of coal under the action of supercritical $CO_2$ and demonstrated that, after the action of supercritical $CO_2$, honeycomb-like pore cracks appeared in coal samples and permeability was significantly improved. In a $CH_4$ experiment in supercritical $CO_2$-flooded coal, it was found that the injection of supercritical $CO_2$ into the coal seam can improve the recovery of $CH_4$ and effectively seal in $CO_2$ (Yang et al., 2012; Liang et al., 2014; Wu et al., 2018b).

Scholars at home and abroad have carried out studies of $CO_2$ seepage and adsorption in coal seams, with results indicating that when the temperature exceeds 31.8°C and the pressure exceeds 7.38 MPa, $CO_2$ becomes supercritical and supercritical $CO_2$ has a specific anti-permeability effect on coal seams (Wang and Liang, 2019). Therefore, in this study, nine coal samples from the Xinqiu Mine Area, Fuxin City in the Liaoning Province, China, were tested. Seepage and adsorption experiments of supercritical $CO_2$ injection of raw coal specimens under different injection pressures and temperatures were performed, and the anti-permeability effect of supercritical $CO_2$ on the specimens was studied by comparing the changes in longitudinal wave velocity and permeability before and after supercritical $CO_2$ injection.

## Coal sample preparation and test device

### Coal sample preparation

Coal samples were taken from the Xinqiu Mine Area, Fuxin City, Liaoning Province. Coring equipment was used to drill the

**TABLE 1 Basic physical parameters of the specimen.**

| Sample | L/mm | D/mm | m/g |
|---|---|---|---|
| M01 | 100.2 | 50.1 | 258.06 |
| M02 | 99.8 | 50.0 | 256.87 |
| M03 | 100.3 | 50.1 | 258.06 |
| M04 | 100.1 | 50.1 | 257.16 |
| M05 | 99.8 | 50.0 | 256.87 |
| M06 | 100.2 | 50.1 | 258.06 |
| M07 | 99.9 | 50.0 | 255.07 |
| M08 | 99.8 | 50.0 | 255.01 |
| M09 | 100.0 | 50.1 | 257.88 |

core perpendicular to the bedding direction of the coal seam; the core was then cut into 50 mm*100 mm standard cylindrical specimens. The inclination of the end face was less than 0.1°, as shown in Figure 1. Nine samples with apparent integrity and no visible cracks were selected. The samples were placed in a drying oven at 105°C for 24 h and then covered with cling film after cooling. The specific parameters of the coal samples are shown in Table 1.

## Experimental device

### Permeability experimental device

Permeability measurement was achieved using the steady-state method. The experimental apparatus used to measure permeability is shown in Figure 2. The device included a gas supply, data acquisition, temperature control, and core holder systems. The core holder system included a triaxial core holder, pressure kettle, and flow meter. The gas supply system included high-pressure gas cylinders, booster pumps, air compressors, pressure pumps, and vacuum pumps that provided pressure for the $CO_2$ phase transition to a supercritical state. The data acquisition system consisted of a TP700 data logger and many pressure transducers, each with an accuracy of 0.01 MPa. The temperature control system consisted of a water bath container and many temperature transducers with an accuracy of 0.1°C. The injection pressure was at least 5 MPa lower than the confining pressure to reduce the possibility of hydraulic fracturing within the shales and leakage of liquid from the gap between the rubber sleeve and the sample (Zhang and Yu, 2019).

### Adsorption experimental device

The experimental apparatus used to measure adsorption is shown in Figure 3. The device included a gas supply system, data acquisition system, temperature control system, and adsorption system. The adsorption system included two high-pressure adsorption chambers, and the pressure of the adsorption tank was 0 ~ 60 MPa; other systems were the same as the permeability experimental device. Unlike the seepage experimental apparatus, the adsorption experimental apparatus did not require confining pressure and axial pressure on shale specimens.

# Permeability experiment

## Permeability model

Based on the stable upstream pressure ($p_1$, MPa), downstream pressure ($p_2$, MPa), and volumetric flow rate of the gas (Q, $m^3/s$), the gas permeability was obtained from the expression (Zhao and Yu, 2017):

$$K = \frac{2Qp_0\mu_g LZ}{A(p_1^2 - p_2^2)Z_a}. \quad (1)$$

where K is the permeability, $10^{-15}$ $m^2$; $p_0$ is the standard atmospheric pressure, 0.1 MPa; L is the length of the coal sample, cm; A is the cross-sectional area of the coal sample, $cm^2$; Z is the compressibility factor under the experimental

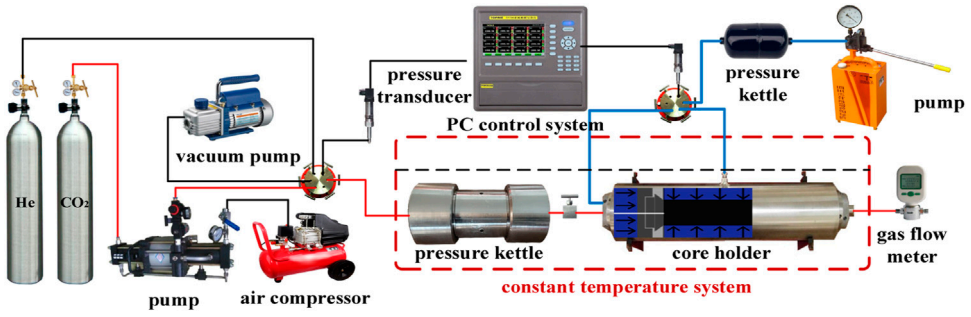


FIGURE 2
Permeability experimental device.

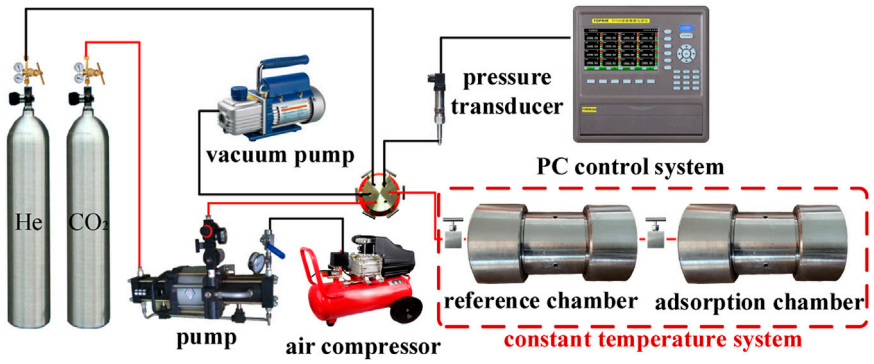


FIGURE 3
Adsorption experimental device.

**TABLE 2 Permeability experiment program.**

| Sample | Temperature/°C | Confining pressure/MPa | Axial pressure/MPa | Pore pressure/MPa |
|---|---|---|---|---|
| M01 | 35 | 12 | 12 | 4–7; 8–11 |
| M02 | 45 | 12 | 12 | 4–7; 8–11 |
| M03 | 55 | 12 | 12 | 4–7; 8–11 |

conditions; and $Z_a$ is the compressibility factor at the experimental temperature.

## Permeability experiment program and steps

The permeability experiments were divided into three groups according to temperature, including 35, 45, and 55°C. The volumetric stress in the experiment was 36 MPa, the $CO_2$ injection pressure was 4–7 MPa, and the supercritical $CO_2$ injection pressure was 8–11 MPa. The experimental program is shown in Table 2. The specific steps were as follows:

1) The test device was connected and confirmed to be airtight. The sample was sealed with a heat shrink sleeve and put into the core holder. The water bath tank temperature was set to 35°C, and the volume stress was set to 36 MPa. After the temperature and pressure stabilized, the pore pressure was adjusted to 4 MPa by feeding $CO_2$, and test data were recorded after allowing the flow to stabilize. Three sets of data were collected for each experimental group, and the average value was calculated.
2) After testing at one observation point, the $CO_2$ injection pressure was gradually increased until 11 MPa, according to the experimental protocol.
3) The coal sample was replaced according to the experimental protocol, and the test temperature was increased to 45°C and then 55°C, in turn. Steps 1) and 2) were repeated, and the coal sample permeability under different test conditions was calculated using the collected data.

## Permeability experiment results and discussion

As shown in Figure 4, under the same volumetric stress, pore pressure and temperature had significant effects on the permeability of coal samples. The permeability of coal samples increased with increased pore pressure at the same temperature, and the permeability increased exponentially before the supercritical state. After the critical pressure was exceeded, the permeability had an obvious linear growth trend. By comparing the permeability of coal samples under the two carbon dioxide phase states, it was found that when the carbon dioxide reached the supercritical state, permeability was significantly improved. Comparing permeability at the three temperatures, it was found that coal permeability was highest and had the smallest decrease in permeability over time at 35°C. These results indicate that the volume of pores and cracks in the coal body was limited. With increased temperature, the expansion of the coal body

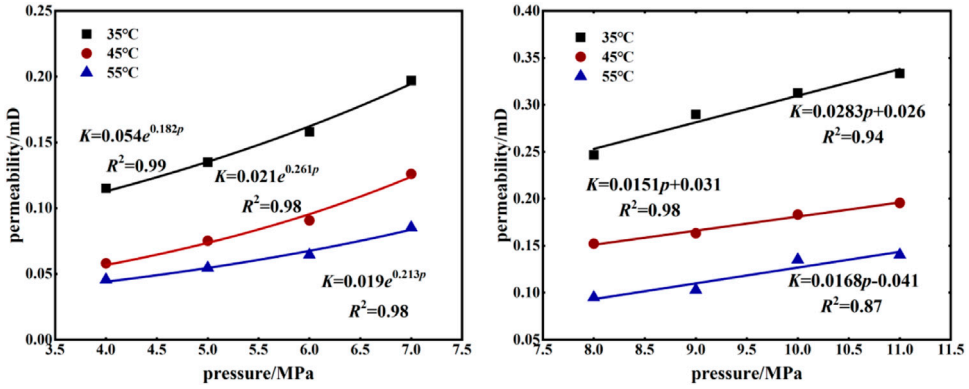


FIGURE 4
Change curves of permeability with an injection of $CO_2$ and SC-$CO_2$ pressure.

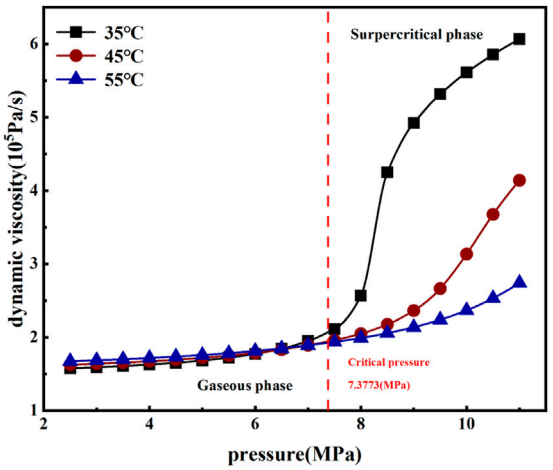


FIGURE 5
Dynamic viscosity of $CO_2$ varies with pressure.

skeleton gradually increases. However, due to the compressive and restrictive effects of effective stress on pore cracks, the volume of pores and fractures gradually decrease with increased expansion of the coal skeleton. The expansion of the coal skeleton will not increase indefinitely with increased temperature. As temperature increases, the rate of change of the expansion of the coal skeleton gradually decreases; i.e., the rate of change of the volume of pores and fractures will gradually decrease. On the other hand, permeability is also related to gas dynamic viscosity. From Eq. 1, the permeability is proportional to the dynamic viscosity of the gas. As shown in Figure 5, comparing the dynamic viscosity of carbon dioxide at three temperatures, it was clear that the dynamic viscosity of $CO_2$ increased with increasing temperature before the supercritical state. The dynamic viscosity of $CO_2$ at 35°C was significantly higher than that at 45°C and 55°C, although, with increased temperature, the viscosity of supercritical $CO_2$ will decrease significantly. The expansion of clay minerals in the coal body plays a leading role in this process (Wu et al., 2018b); therefore, the decrease of permeability will gradually slow down.

# Adsorption experiment

## Adsorption capacity model

After measuring the pressure in the adsorption system before and after adsorption equilibrium, the adsorption amount was calculated based on the change in the number of substances converted using the gas state equation. A known amount of adsorption gas was injected into the reference chamber and the adsorption chamber, and after stabilization, the reference chamber pressure, $p_1$, and the adsorption chamber pressure, $p_2$, were recorded. Using the gas compressibility factor equation of state: $pV = ZnRT$, the amount of gas in the reference chamber, $n_1$, and the amount of gas in the adsorption chamber, $n_2$, were calculated. The valve between the adsorption chamber and the reference chamber was opened, the final equilibrium pressure, p0, was recorded, and the gas factor state equation was used to calculate the total amount of gas, $n_0$, in the adsorption system. The adsorption amount of the gas at this pressure is then: $n_{ad} = n_1 + n_2 - n_0$, and the excess adsorption amount $V_{ad}$ of $CO_2$ per unit mass of coal was calculated using (Eq. 2).

$$V_{ad} = 22.4 \times 10^3 n_{ad} / G_c. \quad (2)$$

In Eq. 2, $G_c$ is the total mass of the coal sample, g.

**TABLE 3 Adsorption experiment program.**

| Sample | Temperature/°C | Pore pressure/MPa |
|---|---|---|
| M04 | 35 | 1–11 |
| M05 | 45 | 1–11 |
| M06 | 55 | 1–11 |

## Adsorption experiment program and steps

Experiments were divided into three groups according to temperatures of 35, 45, and 55°C. The $CO_2$ pressure was gradually increased from 0 MPa to 11 MPa for a total of 11 pressure measurement points, each with a balanced time of not less than 24 h (Tang et al., 2018). The experimental program is shown in Table 3. The specific steps are as follows:

1) Coal samples that had undergone a 35°C seepage test were placed in an adsorption tank, which was heated to 35°C, and then placed in a water bath tank. Helium gas was introduced to bring the pressure in the test system to 11 MPa. Stability of gas pressure was observed for 24 h to ensure the test system was airtight.
2) The volume of free space was measured. Helium gas was passed in to achieve a pressure of 2–3 MPa, and the aforementioned steps were repeated two times. Measurement of free space volume was repeated three times. The difference between the test values of free space volume in the adsorption chamber was less than 0.1 $cm^3$.
3) The vacuum pump was turned on to remove excess gases from the system and vacuum treatment continued for at least 12 h. When the data logger consistently displayed the same data, vacuum treatment was complete.
4) The reference chamber was filled with $CO_2$ gas, and the reference chamber pressure after stabilization was recorded. The balance valve between the reference chamber and the adsorption chamber was opened and kept open for 12 h, and the final balance pressure was recorded. When the adsorption test of one measurement point was completed, introduction of $CO_2$ gas was continued to allow the pressure in the test system to reach 2 MPa, and the aforementioned process was repeated. The test pressure measurement point was 11 MPa, and when the pressure in the test system reached 11 MPa, testing of the group was complete.
5) The test temperature and test specimen were changed and steps 3) and 4) were repeated. The amount of $CO_2$ gas adsorption under different temperature conditions was calculated.

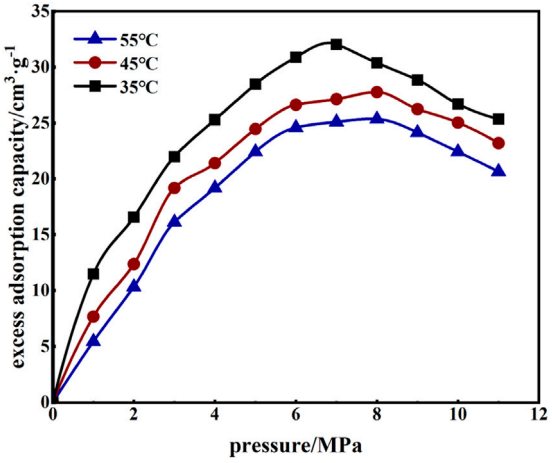


FIGURE 6
Change curves of excess $CO_2$ adsorption with pore pressure.

## Adsorption experiment results and discussion

As shown in Figure 6, under different temperature conditions, the excess adsorption of $CO_2$ by coal samples first increased with the increase of pore pressure. Then, when the pressure reached 6 MPa, the excess adsorption increase decreased significantly, and, at 7–8 MPa, the excess adsorption reached the maximum and then decreased with increased pore pressure. When the temperature was increased from 35°C to 45°C and then 55°C, the maximum excess adsorption of $CO_2$ in coal samples decreased from 31.96, to 27.86, and 25.6 $cm^3/g$, respectively.

From the test data, it was found that for every 10°C increase in temperature, the excess adsorption volume decreased by an average of 8.3%. These data demonstrate that with increased temperature, the $CO_2$ molecules had more energy which, when free from the bondage of the adsorption site, resulted in a decreased amount of adsorption.

In the coal sample adsorption $CO_2$ test, the Langmuir adsorption model is commonly used. However, when $CO_2$ reaches a supercritical state, the Langmuir adsorption model fits poorly, and even the fit result does not converge. Therefore, the Sakurovs modified D-R model (Sakurovs et al., 2007) was used in this study, as it can be applied to the adsorption of supercritical $CO_2$ by converting the adsorption pressure to density and adding a correction coefficient. The specific model is as follows:

$$V_{ad} = V_0\left(1 - \frac{\rho_g}{\rho_a}\right)\exp\left\{-D\left[\ln\left(\frac{\rho_a}{\rho_g}\right)\right]^2\right\} + k\rho_a, \quad (3)$$

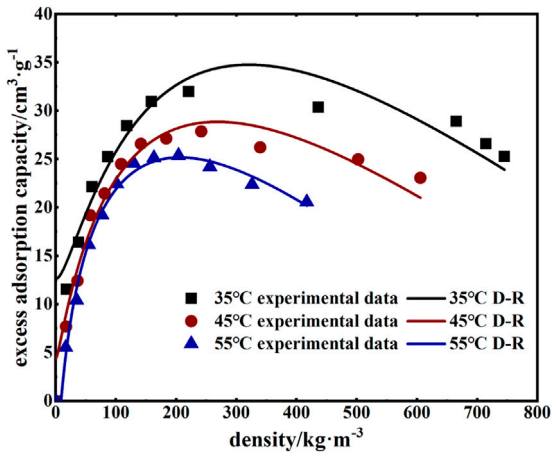


FIGURE 7
D–R model fitted curves of excess $CO_2$ adsorption.

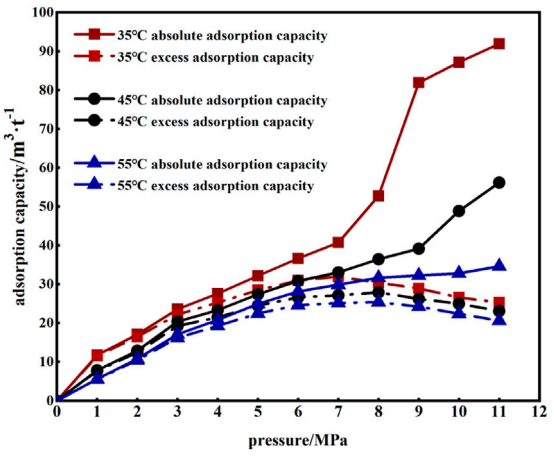


FIGURE 8
Change curves of $CO_2$ adsorption with pore pressure.

**TABLE 4 D-R model fitting parameters.**

| Temperature/°C | $V_0$/cm³·g⁻¹ | D | k | $R^2$ |
|---|---|---|---|---|
| 35 | 34.74 | 0.194 | 0.012 | 0.95 |
| 45 | 28.84 | 0.132 | 0.004 | 0.97 |
| 55 | 25.14 | 0.078 | 0.008 | 0.99 |

where $V_0$ is the maximum excess adsorption under ideal conditions, cm³/g; $\rho_g$ is the density of the adsorbed gas at the corresponding temperature and pressure, kg/m³; $\rho_a$ is the adsorption phase density, and the current common value is 1028 kg/m³ (Li et al., 2014); D and k are constants. The experimental data were collated and then fit using the model mentioned previously; the results are shown in Figure 7 and Table 4.

The fit results demonstrated that the modified D-R model better described the adsorption of supercritical $CO_2$ by coal, with a coefficient of determination $R^2$ that was greater than 0.95 and increased with increasing temperature. The temperature was increased from 35°C to 45°C and then 55°C, corresponding to maximum excess adsorption of 34.74, 28.84, and 25.14 cm³/g, respectively; supercritical $CO_2$ density of 317, 266, and 199 kg/m³, respectively; and supercritical $CO_2$ pressure of 7–9 MPa.

Due to the high test pressure, the excess adsorption does not reflect the true adsorption of $CO_2$ in coal (Yang et al., 2011). Therefore, the absolute adsorption amount $V_{ap}$ was used in this study to describe the amount of $CO_2$ adsorption in coal and was calculated as follows (Moffat and Weale, 1955):

$$V_{ap} = \frac{V_{ad}}{\left(1 - \rho_a/\rho_g\right)}. \quad (4)$$

Under different temperature conditions, the excess adsorption of $CO_2$ and the absolute adsorption amount of coal changed with pore pressure, as shown in Figure 8. When $CO_2$ did not reach the supercritical state, the excess adsorption of $CO_2$ and absolute adsorption under different temperature conditions were consistent, and the absolute adsorption was increased by an average of 16% compared with the excess adsorption (Figure 8).

When $CO_2$ reached a supercritical state, the excess adsorption amount began to decrease with increased pore pressure. In contrast, the absolute adsorption amount increased with increased pore pressure, and the lower the temperature, the more obvious the increase. The supercritical $CO_2$ pressure was 8–11 MPa, and the absolute adsorption amount was increased by an average of 214%, 79%, and 41% compared with the excess adsorption amount, respectively.

## Supercritical $CO_2$ permeability enhancement results and discussion

To better explore the permeability enhancement effect of supercritical $CO_2$ on raw coal samples, the permeability calibration test was applied before and after $CO_2$ treatment, and the change in ultrasonic wave velocity before and after $CO_2$ treatment was assessed.

### Permeability enhancement test

The permeability enhancement effect of supercritical carbon dioxide on coal was analyzed by comparing the $N_2$ permeability of coal samples before and after permeability enhancement. The specific test plan is shown in Table 5, and the experimental steps are

**TABLE 5 Permeability enhancement experiment program.**

| Sample | Temperature/°C | Axial pressure/MPa | Confining pressure/MPa | Time/h |
|---|---|---|---|---|
| M07 | 35 | 12 | 12 | 24 |
| M08 | 45 | 12 | 12 | 24 |
| M09 | 55 | 12 | 12 | 24 |

**TABLE 6 Comparison of P-wave velocity $V_P$ before and after being subjected to supercritical $CO_2$.**

| Temperature/°C | 35 | 45 | 55 |
|---|---|---|---|
| Before $V_P$/(km·s$^{-1}$) | 2.13 | 2.07 | 2.10 |
| After $V_P$/(km·s$^{-1}$) | 1.92 | 1.93 | 1.98 |
| $\Delta V_P$/(km·s$^{-1}$) | 0.21 | 0.14 | 0.12 |

the same as those described in the *Permeability experiment program and steps* section. The experimental results are shown in Figure 8.

As shown in Figure 8, the permeability of coal samples before and after permeability enhancement increased exponentially as the pore pressure increased. After using supercritical $CO_2$ to increase the permeability of coal samples, the permeability of coal samples under the same pore pressure conditions was significantly improved, with an average increase of 53.34%. The greater the pore pressure, the greater the permeability of coal samples, indicating that supercritical $CO_2$ had a good permeability enhancement effect on coal samples.

## Changes in ultrasonic wave velocity

A non-metal detector was used to measure the propagation velocity of longitudinal waves in coal samples before and after the test, as shown in Table 6. After the action of supercritical $CO_2$, the propagation rate of longitudinal waves in the coal sample was significantly slower, and the wave velocity decreased as humidity increased (Table 6). The propagation speed of ultrasonic waves was different in different media; specifically, the propagation speed of solid media was significantly more than that of gaseous media. After the test, the wave velocity slowed, indicating that the coal sample had either a new pore crack or expansion of the original pore crack after the supercritical $CO_2$ action; the lower the temperature, the more obvious the effect. The aforementioned results show that supercritical $CO_2$ promoted the development of coal-like pore fractures, improved the pore connectivity in the coal sample, changed the seepage path of the fluid in the coal sample, and increased the permeability of the sample. Additionally, supercritical $CO_2$ at 35°C had the best enhancement effect on coal sample permeability.

# Conclusion

1) Under the condition of constant volume stress, pore pressure and temperature had a significant impact on the permeability of the coal seam. When the pore pressure was fixed, the permeability decreased with increased temperature; when the temperature was fixed, the permeability increased with increased pore pressure. The injection of supercritical $CO_2$ increased permeability by an average of 93% compared to the permeability of coal samples after $CO_2$ injection.
2) Using the modified D-R model, the adsorption data were fitted and the maximum amount of excess adsorption of $CO_2$ by coal was found to be 7–9 MPa. The temperature was increased from 35°C to 45°C and then 55°C, corresponding to maximum excess adsorption of 34.74, 28.84, and 25.14 cm$^3$/g, respectively. For every 10°C increase in temperature, excess adsorption decreased by an average of 8.3%.
3) Excess and absolute adsorption of carbon dioxide in coal were assessed. When the $CO_2$ did not reach the supercritical state, the excess adsorption amount and the absolute adsorption amount change trends were consistent, and the absolute adsorption amount was increased by an average of 16% compared with the excess adsorption amount. When $CO_2$ reached a supercritical state, the excess adsorption amount began to decrease with increased pressure, and the absolute adsorption amount increased with increased pressure; the lower the temperature, the more obvious the effect.
4) In comparing the changes in coal sample permeability before and after supercritical $CO_2$ action, it was found that after supercritical $CO_2$ was injected into the coal sample, the pore cracks inside the sample were further developed and permeability increased by an average of 53.34%. These data

indicate that supercritical $CO_2$ had a good permeability enhancement effect on the coal seam.

5) Using a non-metallic detector to measure the change in ultrasonic wave velocity of coal samples before and after supercritical $CO_2$ action, it was concluded that supercritical $CO_2$ at 35°C had the best permeability enhancement effect on coal samples.

## Data availability statement

The original contributions presented in the study are included in the article/Supplementary Material; further inquiries can be directed to the corresponding author.

## Author contributions

YY: conceptualization. JL: data curation, writing—original draft, software. YY: investigation. DW: project administration. WZ: investigation. FM: investigation.

## Funding

This study was supported by the National Natural Science Foundation of China (51974147).

## Conflict of interest

The authors declare that the research was conducted in the absence of any commercial or financial relationships that could be construed as a potential conflict of interest.

## Publisher's note

All claims expressed in this article are solely those of the authors and do not necessarily represent those of their affiliated organizations, or those of the publisher, the editors, and the reviewers. Any product that may be evaluated in this article, or claim that may be made by its manufacturer, is not guaranteed or endorsed by the publisher.

## References

Feng, Z. (2008). *Low permeability of coal seam gas extraction the- ory and application*. China, Beijing: Science Press.

He, W., Liang, W., Zhang, B., Li, Z., and Li, L. (2018). Experimental study on swelling characteristics of $CO_2$ adsorption and storage in different coal rank China. *Journal of China Coal Society*. 43 (5), 1408–1415.doi:10.13225/j.cnki.jccs.2017.1138

Jia, C., Zheng, M., and Zhang, Y. (2012). Unconventional hydrocarbon resources in China and the prospect of exploration and development China. *Petroleum Exploration and Development*. 39 (2), 129–136.doi:10.1016/s1876-3804(12)60026-3

Li, Q., Ni, X., Wang, Y., and Gang, S. (2014). The experi- mental study on the adsorption/desorption of carbon dioxide in the coal under supercritical condition China. *Coal Geology & Exploration*. 42 (3), 36–39.

Liang, W., Zhang, B., Han, J., and Yang, D. (2014). Experi- mental study on coal bed displacement and recovery by super crit-ical carbon dioxide injection China. *Journal of China Coal Society*. 39 (8), 1511–1520.

Ma, L., Li, B., Deng, J., Li, B., and Hu, A. (2015). On the characteristic fea- tures of the adsorption capacity of the coal for the singular compo- nent gases of $CH_4$, $CO_2$, $N_2$ under regular pressures China. *Journal of Environment and Safety*. 15 (2), 64–67.

Miao, F., Wu, D., Liu, X., Xiao, X., Zhai, W., and Geng, Y. (2022). Methane adsorption on shale under *in situ* conditions: Gas-in-place estimation considering *in situ* stress. *Fuel* 308, 121991. doi:10.1016/j.fuel.2021.121991

Moffat, D. H., and Weale, K. E. (1955). Sorption by coal of methane at high pressures China. *Fuel* 34, 449–462.

Qin, Y. (2005). Advances in overseas geological research on coalbed gas: Origin and reservoir characteristics of coalbed gas China. *Frontiers in Earth Science*. 12 (3), 289–298.

Reucroft, P. J., and Patel, H. (1986). Gas-induced swelling in coal. *Fuel* 65 (6), 816–820. doi:10.1016/0016-2361(86)90075-x

Reucroft, P. J., and Sethuraman, A. R. (1987). Effect of pressure on carbon dioxide induced coal swelling. *Energy fuels*. 1 (1), 72–75. doi:10.1021/ef00001a013

Sakurovs, S., Day, S., Weir, S., and Duffy, G. (2008). Temperature dependence of sorption of gases by coals and charcoals. *International Journal of Coal Geology*. 73 (3/4), 250–258. doi:10.1016/j.coal.2007.05.001

Sakurovs, R., Day, S., Weir, S., and Duffy, G. (2007). Application of a Modified Dubinin–Radushkevich Equation to Adsorption of Gases by Coals under Supercritical Conditions. *Energy fuels*. 21, 992–997. doi:10.1021/ef0600614

Sun, K., Wu, D., Su, A., Chen, Z., Ren, S., Yue, L., et al. (2013). Coupling experimental study of coal permeability with pore pressureeffective volume stresstemperature under supercritical carbon dioxide action China. *Chinese Journal of Rock Mechanics and Engineering*. 32 (S2), 3760–3767.

Tang, J., Wang, X., Lu, Y., Ao, X., and Han, S. (2018). Experimental study on time effect and deformation anisotropy of shale and coal under $CO_2$ China. *Journal of China Coal Society*. 43 (8), 2288–2295.

Tang, S., Tang, D., and Qi, Y. (2004). Binary-component gas adsorption isotherm experiments and their significance to ex- ploitation of coalbed methane China. *Earth Science* (2), 219–223.

Wang, L., and Liang, W. (2019). Experimental study on crack propa- gation of coalrock mass under supercritical CO2 fracturing China. *Coal Science Technology*. 47 (2), 65–70.

Wu, D., Miao, F., Liu, X., Xiao, X., and Zhai, W. (2021). Prediction of high-pressure adsorption of CH4 and CO2 in shale. *International Journal of Greenhouse Gas Control*. 110, 103440. doi:10.1016/j.ijggc.2021.103440

Wu, D., Liu, X., Sun, K., Xiao, X., and Xin, L. (2018). Experiments on supercritical CO2 adsorption in briquettes. *Energy Sources, Part A: Recovery, Utilization, and Environmental Effects* 41 (8), 1005–1011. doi:10.1080/15567036.2018.1523258

Wu, D., Liu, X., Liang, B., Sun, K., and Xiao, X. (2018). Experiments on Displacing Methane in Coal by Injecting Supercritical Carbon Dioxide. *Energy fuels*. 32 (12), 12766–12771. doi:10.1021/acs.energyfuels.8b03172

Wu, S., and Zhao, W. (2005). Analysis of effective stress in adsorbed methane-coal system China. *Chinese Journal of Rock Mechanics and Engineering*. 24 (10), 1674–1678.

Wu, S., Tang, D., Song, L. I., and Li, X. (2019). Effect of temperature and pressure on energy parameters of methane supercritical adsorp- tion China. *Coal Science. Technology*. 47 (9), 60–67.

Xu, J., Chen, Y., Jiang, C., Li, C., and Zeng, C. (2017). Test on carbon dioxide permeability in coal seam China. *Ministry of Environment, Forest and Climate Change*. 44 (4), 10–13.

Yang, Z., Qin, Y., Gao, D., and Chen, R. (2011). Differences between apparent and true adsorption quantity of coalbed methane under supercritical conditions and their geological significance China. *Natural gas in India* 31 (4), 13–16.

Yang, T., Nie, B., Yang, D., Zhang, R., and Zhao, C. (2012). Experimental research on displacing coal bed methane with supercritical CO2. *Safety. Science*. 50 (4), 899–902. doi:10.1016/j.ssci.2011.08.011

Zhang, C., and Yu, Q. (2019). Breakthrough pressure and permeability in partially water-saturated shales using methane-carbon dioxide gas mixtures: An experimental study of Carboniferous shales from the eastern Qaidam Basin, China. *Bulletin* 103 (2), 273–301. doi:10.1306/07111818018

Zhao, Y., and Yu, Q. (2017). CO 2 breakthrough pressure and permeability for unsaturated low-permeability sandstone of the Ordos Basin. *Journal of Hydrology* 550, 331–342. doi:10.1016/j.jhydrol.2017.04.050